J|A|C|S
ARTICLES
Published on Web 04/27/2007

Reactivity of Platinum Metal with Organic Radical Anions from Metal to Negative Oxidation States

Jalal Ghilane, Maryline Guilloux-Viry, Corinne Lagrost, Jacques Simonet, and Philippe Hapiot*

Contribution from the Sciences Chimiques de Rennes, UMR N° 6226 CNRS-Université de Rennes 1, Campus de Beaulieu, 35042 Rennes, France

Received March 2, 2007; E-mail: philippe.hapiot@univ-rennes1.fr

Abstract: The reaction of platinum metal with an organic molecular radical anion leads to the formation of iono-metallic phases where Pt exists under negative oxidation states. This puzzling transformation of a "noncorrodible metal" was examined using localized electrochemical techniques in dimethylformamide containing different tetra-alkylammonium salts chosen as test systems. Our experiments demonstrate that the platinum metal is locally reduced as soon as the Pt faces relatively moderate reducing conditions, for example, when the Pt is used as a negative electrode or when the metal is in the presence of a reducing agent such as an organic radical anion. Scanning electrochemical microscopy (SECM) analysis, current−distance curves, and transient mode responses provide detailed descriptions of the reactivity of Pt to form negative oxidation states (the key step is the reaction of the metal with a molecular reducing agent), of the insulating nature of the "reduced" solid phases of the thermodynamics and kinetics conditions of the Pt conversion. The passage from the conductor to insulator states controlled the spatial development of the reaction that always remains in competition with the other "natural" roles of a metallic electrode. Formally, the phenomena can be treated by analogy with the C. Amatore's model previously developed for the mediated reduction of the poly(tetrafluoroethylene). Consequences of this general reactivity of Pt are discussed in view of a wide utilization of this metal in reductive conditions and the possible applications of such processes in the micropatterning of metallic surfaces.

Introduction

Noble metals, especially platinum, are widely used in numerous devices because they are considered as a noncorrodible or inert metal. Despite this generally admitted conclusion, dramatic morphological changes were reported when the platinum metal was simply held at a relatively mild negative potential (around −1.6 V/SCE) in a dry organic solvent, for example in dimethylformamide (DMF) containing inorganic or organic salts used as supporting electrolyte.[1] By analogy with the work of Zintl who, in the beginning of the 20th century, made series of iono-metallic phases,[2,3] the electrochemical transformation observed with platinum was proposed to correspond to the interfacial formation of intermetallic phases with a general formula [Pt^-_n, Cat^+, y CatX], where Cat^+ and X^- are the cation and anion of the supporting electrolyte present in the solution. However, the Zintl (−Klemm) concept has been developed for intermetallic phases involving post-transition metals and assumed a complete transfer of the valence electrons from the more electropositive component to the more electronegative one. In this connection, a few works have reported on the formation of "platinides". Red transparent Cs_2Pt crystals showing full charge separation, Ba−Pt systems (BaPt, Ba_3Pt_2, Ba_2Pt, $BaPt_2$, $BaPt_5$), Ca_3Pt_2 structures or the more complex $Pt_2In_{14}Ga_3O_8F_{15}$ crystal have been described.[4−7] It is worth outlining that the synthesis and isolation of these platinides structures require severe experimental conditions as the salts were obtained in very strong reducing conditions. The existence of negative redox states for Pt was clearly confirmed by XPS-measurements on barium platinides prepared by a similar method. In our case, on the basis of electrochemical and scanning probe microscopy measurements, a similar stoichi-

(1) (a) Cougnon, C.; Simonet, J. *Platinum Met. Rev.* **2002**, *46*, 94. (b) Cougnon, C.; Simonet, J. *Electrochem. Commun.* **2002**, *4*, 266. (c) Cougnon, C.; Simonet, J. *Electroanal. Chem.* **2002**, *531*, 179. (d) Simonet, J. *Platinum Met. Rev.* **2005**, *50*, 180.
(2) (a) Zintl, E.; Woltersdaf, G. Z. *Electrochemistry* **1935**, *41*, 876. (b) Zintl, E.; Dullenkopf, G. Z. *Phys. Chem. B* **1932**, *16*, 183.
(3) Solid phases were obtained upon cathodic reduction of various metals, in nonaqueous solvents containing organic or inorganic background electrolytes according to some complicated reduction processes involving the electrode material. (a) Tomashova, N. N.; Kiseleva, I. G.; Astakhov, I. I.; Kabanov, B. N. *Elektrokhimiya* **1968**, *4*, 471. (b) Teplitskaya, G. L.; Astakhov, I. I. *Elektrokhimiya* **1970**, *6*, 379. (c) Teplitskaya, G. L.; Astakhov, I. I. *Elektrokhimiya* **1972**, *8*, 1199. (d) Baranski, A. S.; Fawcett, W. R. J. *Electrochem. Soc.* **1982**, *129*, 901. (e) Kariv-Miller, E.; Svetlicic, V. J. *Electroanal. Chem.* **1985**, *205*, 319. (f) Kariv-Miller, E.; Andruzzi, R. J. *Electroanal. Chem.* **1985**, *187*, 175. (g) Svetlicic, V.; Kariv-Miller, E. J. *Electroanal. Chem.* **1986**, *209*, 91. (h) Ryan, C. M.; Svetlicic, V.; Kariv-Miller, E. J. *Electroanal. Chem.* **1987**, *219*, 247. (i) Gewirth, A. A.; Niece, B. K. *Chem. Rev.* **1997**, *97*, 1129.
(4) Karpov, A.; Nuss, J.; Wedig, U.; Jansen, M. *Angew. Chem., Int. Ed.* **2003**, *42*, 4818.
(5) (a) Schulz, H.; Ritapal, W.; Bronger, W.; Klemm, W. *Z. Anorg. Allg. Chem.* **1968**, *357*, 299. (b) Karpov, A.; Nuss, J.; Wedig, U.; Jansen, M. *J. Am. Chem. Soc.* **2004**, *126*, 14123. (c) Karpov, A.; Wedig, U.; Dinnebier, R. E.; Jansen, M. *Angew. Chem., Int. Ed.* **2005**, *44*, 770. (d) Karpov, A.; Konuma, M.; Jansen, M. *Chem. Commun.* **2006**, 838.
(6) Palenzona, A. *J. Less-Common Met.* **1981**, *78*, P49.
(7) Köhler, J.; Chang, J.-H.; Whangbo, M.-H. *J. Am. Chem. Soc.* **2005**, *127*, 2277.

10.1021/ja071483a CCC: $37.00

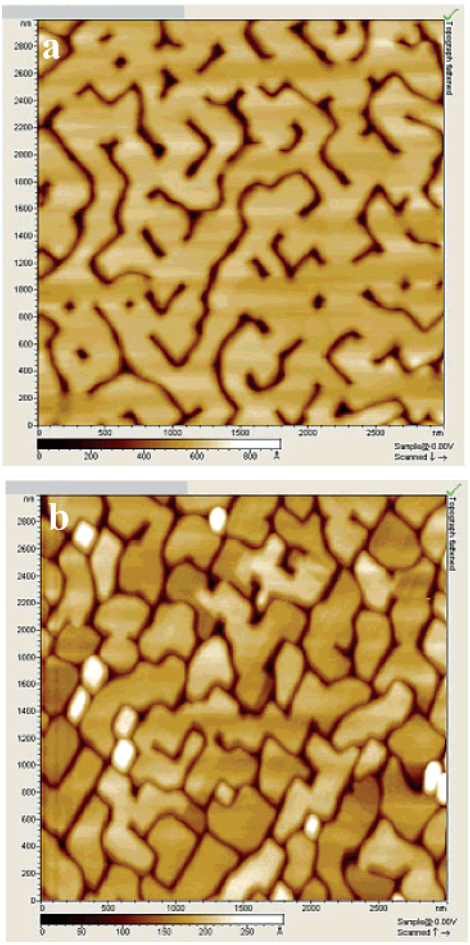

Figure 1. AFM images of platinum substrates: (a) macroscopically conducting substrate; (b) microscopically conducting substrate. Image scans size is $3 \times 3\ \mu m^2$.

ometry during electrochemical treatment was determined in the presence of CsI suggesting that similar types of ionic arrangement could be formed under cathodic polarization. In our recent work, we demonstrated that the same type of negative oxidation states of the Pt is reached during its electrochemical reduction.[8] However, besides these apparent similarities, the energetic conditions required for observing the reducing transformations are totally different. If the formation of Pt with a negative redox state is imaginable in strong reducing conditions, the electrochemical process appears more puzzling. Indeed as highlighted above, in some cases, the electrochemical transformation of Pt is detected as soon as the metal potential becomes more negative than −1.0 V/SCE[1d] which, corresponds to very mild reduction conditions by comparison with the strong reductive power of the metallic Cs.

Electrochemical investigations (cyclic voltammetry, coulometry, electrochemical quartz crystal microbalance EQCM)[9,10] show that this transformation occurs with a large variety of cations and anions and involves electron transfers coupled with the insertion of the electrolyte cation in the metallic lattice:

$$n\mathrm{Pt} + \mathrm{e}^- + 2\mathrm{Cat}^+ + \mathrm{X}^- \rightarrow [\mathrm{Pt}_n{}^-, \mathrm{Cat}^+, \mathrm{CatX}]$$

The increase of volume due to this process leads to impressive morphological modification for which the shape, stability, and reversibility were found to largely depend on the nature of CatX, electrode potential, or initial structure of the platinum.[10c] These electrogenerated platinum phases exhibit some efficient reductive properties that can be used for locally inducing electrochemical-grafting reactions like those based on the reduction of aryldiazonium salts.[11] Additionally, the existence of such a reductive process appears quite general and not limited to intermetallic salts. As reported in our previous work,[10c] the structural modifications were detected after the electrochemical treatment when the cation Cat^+ was an alkali metal but also with organic cations (for example large tetraalkylammonium cation).

All these previous observations lead us to investigate, in more details, this perplexing reaction that should correspond to some special reactivity of the Pt metal. Moreover, because of the large use of Pt as noncorrodible cathodic material, we may also wonder about its possible intervention in several interfacial processes.

In the present study the reactivity of Pt metal was investigated with a large variety of reducing agents, like radical anion, $M^{\bullet -}$. To examine the generality of this platinum reaction that goes far behind the electrochemical formation of intermetallic salts, we focused our investigations on the more puzzling case where the cation involved in the reaction is an organic cation like an alkylammonium R_4N^+ (R = ethyl, *n*-butyl, *n*-octyl):

$$n\mathrm{Pt} + \mathrm{M}^{\bullet -} + 2\mathrm{R_4N}^+ + \mathrm{BF_4}^- \rightarrow [\mathrm{Pt}_n{}^-, \mathrm{R_4N}^+, \mathrm{R_4NBF_4}] + \mathrm{M}$$

This reaction was investigated using scanning electrochemical microscopy (SECM) which is an appropriate tool for examining the reactivity of the substrate, Pt metal in our case, with a large variety of reactants. This electrochemical technique is based on the formation of a reactant, here a stable radical anion $M^{\bullet -}$, at a probe tip located in the vicinity of the Pt substrate and on the simultaneous observation of the interactions of this species with the substrate through the variation of the current at the probe electrode. Thus, despite the electrochemical generation of reactants, the data provide a direct observation of the chemical reaction between the reactant and the platinum substrate in the solution.

Experimental Section

Reagents. All in situ investigations (SECM, EC-AFM) were performed in dry *N*,*N*-dimethylformamide DMF (puriss, Fluka) stored over molecular sieves. A series of tetraalkylammonium salts were chosen to vary the size of the cation (NEt_4, NBu_4, $NOct_4$), from Fluka (Puriss, Electrochemical grade) and used at concentrations at 0.1 $mol \cdot L^{-1}$. The redox mediators used in the SECM experiments were purchased from Aldrich at the highest available purity and used as received. All solutions were deaereted with argon bubbling prior to each measurement, and experiments were performed in an environmental chamber filled with argon.

(8) Ghilane, J.; Lagrost, C.; Guilloux-Viry, M.; Simonet, J.; Delamar, M.; Mangeney, C.; Hapiot, P. J. *J. Phys. Chem. C* **2007**, *111*, 5701.
(9) (a) Simonet, J.; Labaume, E.; Rault-Berthelot, J. *Electrochem. Commun.* **1999**, *1*, 252. (b) Cougnon, C.; Simonet, J. *Electrochem. Commun.* **2001**, *3*, 209.
(10) (a) Bergamini, J.-F.; Ghilane, J.; Guilloux-Viry, M.; Hapiot, P. *Electrochem. Commun.* **2004**, *6*, 188. (b) Cougnon, C.; Simonet, J. *Electroanal. Chem.* **2001**, *507*, 226. (c) Ghilane, J.; Guilloux-Viry, M.; Lagrost, C.; Hapiot, P.; Simonet, J. *J. Phys. Chem. B* **2005**, *109*, 14925.
(11) Ghilane, J.; Delamar, M.; Guilloux-Viry, M.; Lagrost, C.; Mangeney, C.; Hapiot, P. *Langmuir* **2005**, *21*, 6422.

Substrate Preparation. Platinum samples were prepared by dc sputtering of Pt, applying a voltage of −2.3 KV, under argon pressure of 5.10^{-2} mbar, onto MgO(100) single-crystal substrates heated at 450 °C. Distributions of Pt(100) platelets were obtained with 100−200 nm surfaces and an average thickness around 50 nm. The high crystalline quality of the film was checked by X-ray diffraction showing the (100) orientation of the Pt films and evidencing the epitaxial growth of the Pt films.[12] We have previously shown that this type of structured sample allows clean observation and control of the surface electrode by AFM.[10a] By adjusting the experimental conditions, different general patterns could be obtained where the platinum areas are connected or not. For EC-AFM experiments, the preparation conditions were adjusted to create connected Pt areas so that the sample was macroscopically conducting and behaved like a single massive electrode (see Figure 1a).[10a,c] For SECM experiments to limit the lateral diffusion of the modification, different conditions of preparation were chosen for which the Pt areas were not connected (see Figure 1b) resulting in that the sample is microscopically conducting and macroscopically insulating.

Electrodes. Disk ultramicroelectrodes (UMEs) with a 10 μm-radius were made by sealing gold wire (Goodfellow) in a soft glass tube that was subsequently ground at one end and by following previously published procedures.[13] The glass sheaths were conically shaped with an outer diameter of approximately 100 μm ($5 < RG < 10$). Prior to use, the UME was polished using decreasing-sized diamond pastes. A homemade electrochemical cell was used for the SECM experiments. The reference electrode was a quasi-reference electrode made with an Ag wire covered with $AgNO_3$. Its potential was checked versus the ferrocene/ferrocenium couple (considering $E° = 0.400$ V/SCE), and all potentials were referenced against the SCE reference electrode. A platinum wire (0.5 mm diameter) was used as the auxiliary electrode.

Electrochemical Measurements. SECM experiments were performed with a homemade SECM for which details were previously described in the literature.[14] The potentiostat was a PAR model M273 (EG&G). In the present experiments, the UME tip was moved by a horizontal translation stage at a 2 μm/s speed. The SECM data, approach curves, are plotted as the normalized current (I_T = approach current tip i_T/steady-state current i_{inf}) versus the normalized distance $L = d/a$, where d is the distance between the tip and the substrate and a is the radius of the tip. These curves were produced, in electrolyte solution containing the redox mediator (concentration 5−10 mM), by holding the potential of the UME at the reduction plateau of the mediator (typically 200−300 mV after the half-wave potential). To verify that the active surface of the gold UME is not modified in our experimental conditions, even for the most negative mediators, we checked that the steady-state plateau current of the mediator reduction remained stable before and after the SECM experiments. The planarity of the sample was tuned by recording three approach curves from three different positions located on a triangle of the sample and adjusting the height position of the samples until all the approach curves are similar.

For SECM experiments performed in transient mode, we use a sample of MgO covered by a thin layer of Pt(100) where half of the substrate was masked before the metal deposition. By this way, the same sample contains a covered (platinum) and an uncovered (MgO insulating) area; this difference is useful to position the tip near the substrate (8 μm) with high resolution. Typically, the approach curve is first recorded with the tip located over the insulator area, and the movement is stopped when the normalized current reaches the value $i_t/i_{inf} = 0.4$; this value of current corresponds to a separate distance

Scheme 1. Schematic of SECM Configuration for Localized Modification of Platinum Substrate[a]

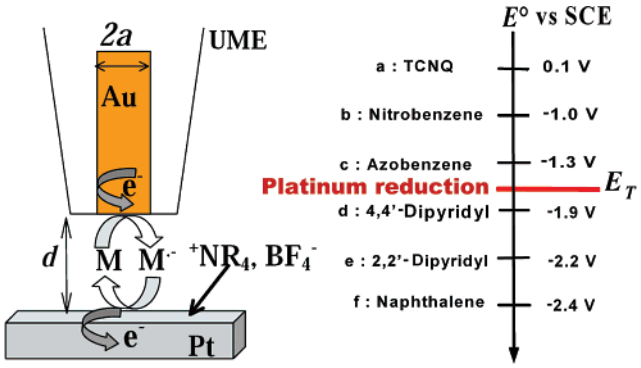

[a] E_T is the threshold potential of platinum reduction = −1.6 V/SCE.

substrate tip around 8 μm. Then, the tip is laterally moved in the area covered by the platinum, and the step potential is applied during 50 s to ensure the reduction of the mediator.

AFM Experiments. The morphology of the platinum modifications was characterized by contact-mode atomic force microscopy using PicoSPM II with a 100 μm range scanner from Molecular Imaging (Tempe, Arizona). In this microscope, the scanner carrying the Si_3N_4 cantilevers is located beneath the sample (top-down scanning). All the AFM images were carried in DMF solution.

Results and Discussion

Steady-State SECM Experiments. The electrochemical cathodic modifications of a thin layer of platinum in dimethylformamide (DMF) in the presence of an alkali metal cation or a tetraalkylammonium salt when using EC-AFM were previously observed. This technique allows the in-situ observations of the topology changes during the process.[10] The recorded images display large morphological transformations associated with the electron transfer. Small grains covering the platinum surface became visible and progressively grew up upon the injected charge leading to a new topography completely different to the initial surface. In the case of NR_4BF_4 salts, the appearance of these small grains starts at threshold potential $E_T = -1.6$ V/SCE (the E_T is defined as the potential where the variation of current is observed; typically this value correspond to the potential where the current value is around 1/20 of the peak current). This potential value is in agreement with the cyclic voltammetry experiments made with a massive Pt electrode dipped in the same solvent and supporting electrolyte. Additionally, both electrochemical and structural reversibility of the reduced phase were proved.[10c] Scanning electrochemical microscopy (SECM) offers a different and unique way of investigation, as the process is induced from the solution side through a chemical reaction between the Pt metal and the electrogenerated radical anion.[15] The key step is the reaction between the electrogenerated radical-anion with the metallic surface. We used the basic principle of the feedback mode of SECM in steady-state mode as presented on Scheme 1.

In this setup, the Pt layer is not electrically connected (unbiased substrate). Effectively, to achieve the SECM experiments, it is not possible to polarize the Pt substrate: a polarization of the substrate at a negative potential would result

(12) Duclère, J. R.; Guilloux-Viry, M.; Perrin, A.; Cattan, E.; Soyer, C.; Rèmiens, D. *Appl. Phys. Lett.* **2002**, *81*, 2067.
(13) Andrieux, C. P.; Hapiot, P.; Pinson, J.; Savéant, J.-M. *J. Electroanal. Chem.* **1988**, *243*, 321.
(14) Ghilane, J.; Hauquier, F.; Fabre, B.; Hapiot, P. *Anal. Chem.* **2006**, *78*, 6019.
(15) (a) Fan, F.-R. F.; Bard, A. J. *Science* **1995**, *267*, 871. (b) Fan, F.-R. F.; Kawak, J.; Bard, A. J. *J. Am. Chem. Soc.* **1996**, *118*, 9669.

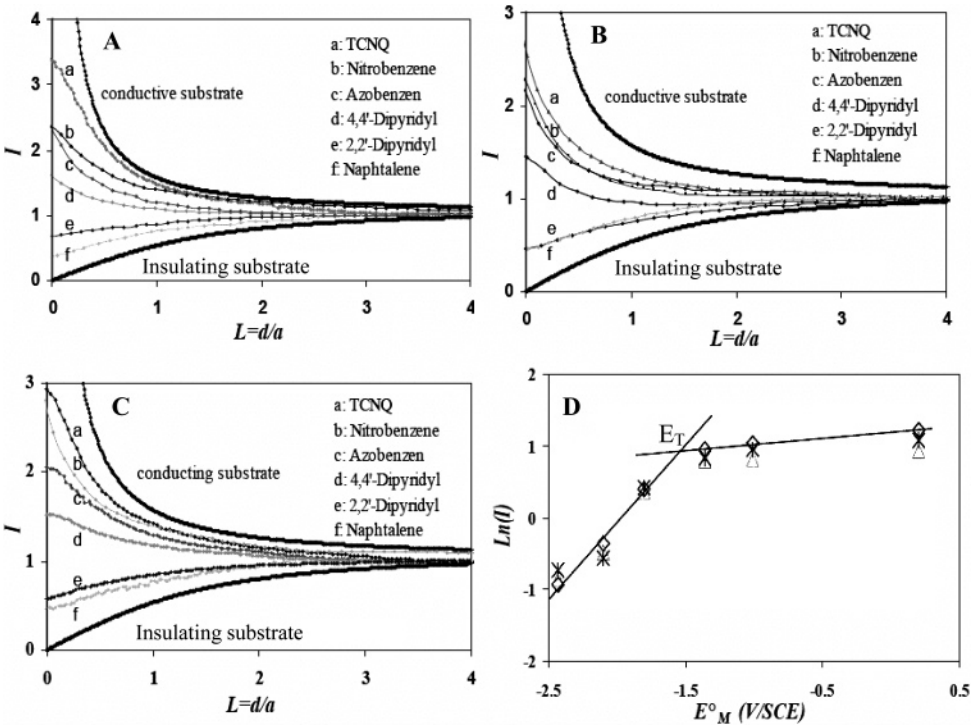

Figure 2. (A) Approach curves using Et_4NBF_4; (B) approach curves using *n*-Bu_4NBF_4; (C) approach curves using *n*-Oct_4NBF_4; (D) variation of the substrate reduction current *I*, obtained at a tip−substrate distance of 0.1*a*, with the standard reduction potential of the redox mediator, (◇) tetraethylammonium, (Δ) tetrabutylammonium, (∗) tetraoctylammonium tetrafluorobate salts.

in the direct electrochemical reduction, and on the contrary a polarization at a positive potential would lead to the reoxidation of the electrogenerated phase.

The probe tip (10 μm radius UME) is placed in a desoxygenated solution containing a redox mediator ($M/M^{\bullet-}$) and the different quaternary ammonium salts NR_4BF_4 (R = ethyl, butyl, octyl). Six different mediators were chosen, the standard potential of the first three mediators are more positive than E_T, while the other are more negative than E_T. These series of experiments provide a unique way for investigating the influence of the driving force through the choice of the redox potential of the mediator and the nature of the tetraalkylammonium salts.[16,17] Figure 2 panels A−C show the experimental approach curves recorded for the different supporting electrolytes and for several radical anions, $M^{\bullet-}$, electrogenerated at the UME approaching a virgin platinum substrate. The approach curves represent the variations of the normalized current (I_T = approach current tip i_T/steady-state current i_{inf}) versus the normalized distance $L = d/a$, where *d* is the distance between the tip and the substrate, and *a* the radius of the tip (feedback mode).[18] The steady-state current i_{inf} is given by the following equation: $i_{inf} = 4nFDCa$ (*n* represents the number of charges transferred per species, *F* is the Faraday constant, *D* and *C* are the diffusion coefficient and concentration for the electrochemically active species in solution, respectively, and *a* is the active radius of the UME). When the distance between the tip and the Pt substrate is close to the order of the electrode radius (a few micrometers), the reduced mediator ($M^{\bullet-}$) diffuses to the liquid−solid interface, where it can react (or not) with the Pt substrate inducing a modification of the faradic tip current. As seen in Figure 2A−C, for $d/a > 3$, all the approach curves are similar and can be almost superposed, proving the absence of interaction between the radical anion and the Pt substrate at long distance. When $d < 3a$, that is, when $M^{\bullet-}$ starts to interfere with the Pt surface, two different situations could be distinguished according to the standard potential reduction of the mediator, $E°_{M/M^{\bullet-}}$. For the weakest reducing $M^{\bullet-}$ (mediators a, b, and c), one can observe that the dimensionless current $I_T = i_T/i_{T,\infty}$ increases corresponding to a positive feedback. These responses are in agreement with the "normal" behavior predicted for conductive metallic platinum and simply correspond to the rapid oxidation of the radical anion on a metallic substrate (regeneration of the mediator) (see Schemes 1 and 2A). On the contrary, for the strongest reducing $M^{\bullet-}$ (mediators d, e, and f), an unexpected decreases of I_T is observed. The current attenuation is proportional to the separate distance *d*, and the overall approach curves evidence a negative feedback.

The drop off of the current indicates the absence of regeneration of the mediator at the platinum surface and tends to the behavior expected for an insulator surface. This tendency is more pronounced when the standard potential of the mediator becomes more negative (i.e., when the radical anion exhibits a stronger reducing character). This phenomenon leads to a considerable modification of the chemical nature of the Pt substrate which becomes insulating. These observations can be rationalized with the following set of reactions:

At the tip UME

$$M + e^- \rightarrow M^{\bullet-} \qquad E°_{M/M^{\bullet-}} \qquad (I)$$

(16) Bard, A. J.; Fan, F.-R. F.; Mirkin, M. V. In *Electroanalytical Chemistry*; Bard, A. J., Ed.; Marcel Dekker: New York, 1994; Vol. 18, pp 243−373.
(17) *Scanning Electrochemical Microscopy*; Bard, A. J., Mirkin, M. V., Eds.; Marcel Dekker: New York, 2001.
(18) (a) Unwin, P. R.; Bard, A. J. *J. Phys. Chem.* **1991**, *95*, 7814. (b) Zhou, F.; Unwin, P. R.; Bard, A. J. *J. Phys. Chem.* **1992**, *96*, 4917. (c) Demaille, C.; Unwin, P. R.; Bard, A. J. *J. Phys. Chem.* **1996**, *100*, 14137. (d) Zhou, F.; Bard, A. J. *J. Am. Chem. Soc.* **1994**, *116*, 393. (e) Treichel, D. A.; Mirkin, M. V.; Bard, A. J. *J. Phys. Chem.* **1994**, *98*, 5751.

Scheme 2. Competition between Pt Reduction and Mediator Regeneration

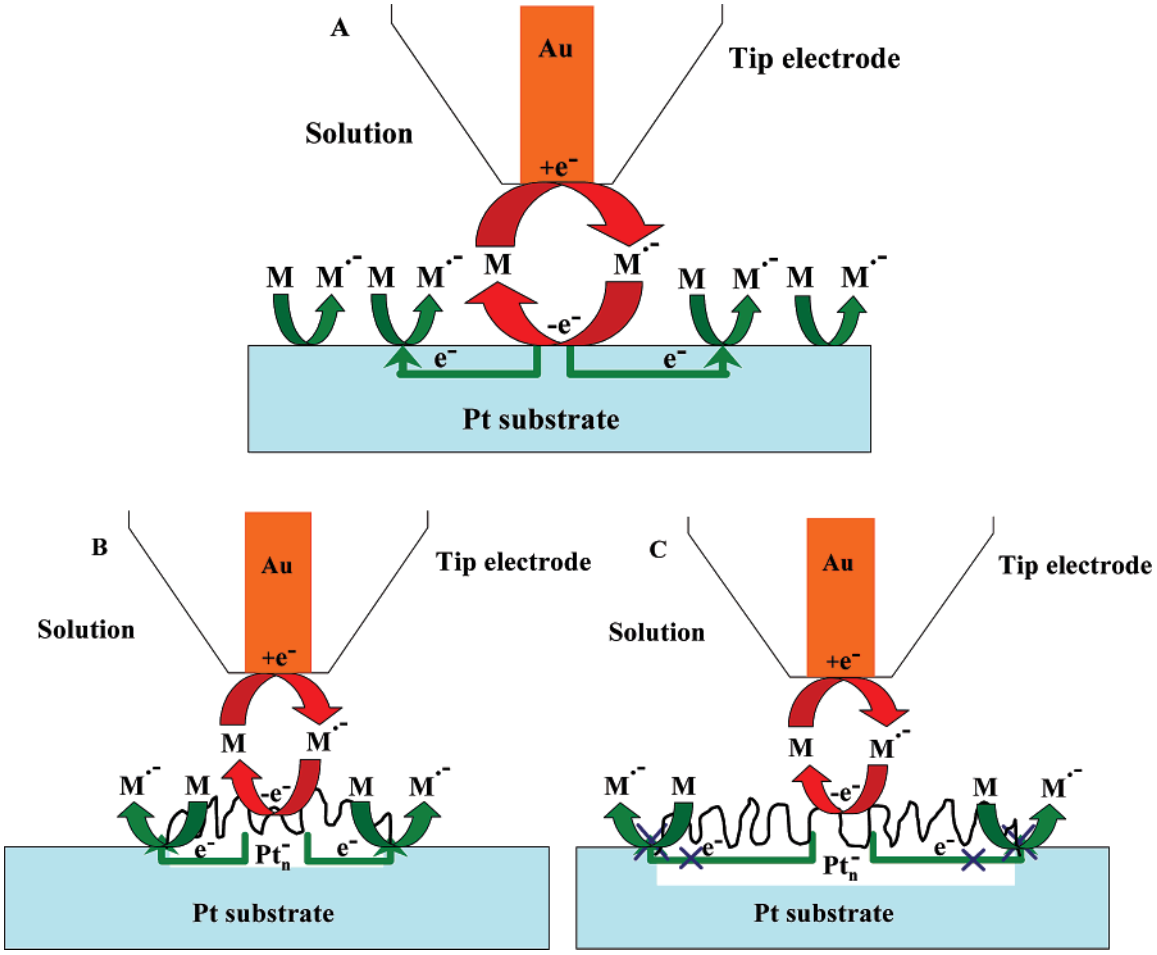

At the platinum substrate

$$Pt + M^{\bullet -} \rightarrow Pt + M + e^- \qquad \text{(II)}$$

$$E^\circ_{M/M^{\bullet -}} > E_T, \quad \text{mediators a, b, and c}$$

$$n\text{Pt} + M^{\bullet -} + 2R_4N^+ + BF_4^- \rightarrow [\text{Pt}_n^-, R_4N^+, R_4NBF_4] + M \qquad \text{(III)}$$

$$E^\circ_{M/M^{\bullet -}} < E_T, \quad \text{mediators d, e, and f}$$

In this chemical scheme, the radical anion of the mediator is electrogenerated at the UME (reaction I). When the distance between the UME and the substrate of platinum is small enough (few μm, $d < 3a$), the radical anion interferes with the platinum substrate. For the mediators (a, b, and c), any change of the chemical nature of the platinum surface is not observed as indicated by the positive feedback; the radical anion is simply exchanging an electron with a metallic surface and is not reactive enough for inducing the modification (reaction II). If the reducing power of the radical anion is sufficient to induce the reduction of Pt (mediator d, e, and f), the cathodic modifications of the platinum surface become possible, which lead to the formation of the reduced organo-metallic phases (reaction III).[19] As attested by our experiments, this phase is electrically insulating and, in steady-state conditions, rapidly leads to a blocking effect of the oxidation of $M^{\bullet -}$ to M. From this point, we can conclude that an organic radical anion with a reducing power stronger than E_T is able to "reduce" platinum. This reduction process has as consequence: the change of the chemical nature of the platinum from conducting material to an insulating one.

To complete the experiments, the topography of the platinum substrate was imaged by AFM after the SECM approach experiments. During these experiments, the substrate is kept in the original solution under argon atmosphere to avoid the chemical oxidation of the "reduced Pt" by air. Thus, Figure 3a displays the topography of the freshly prepared platinum substrate on a large area of 100 μm × 100 μm. At this scale, the sample appears as a flat surface and, as expected, demonstrates the stability of the platinum after contact with a DMF solution containing the mediator and the supporting electrolyte. After the SECM experiments, when the mediator was the naphthalene/naphthalene radical anion couple and the supporting electrolyte the tetrabutylammonium salt (Figure 3b) or tetraoctylammonium (Figure 3c), some considerable modifications of the surface topography are visible and localized on a roughly circular area around 80 μm diameter, which corresponds to four times the tip electrode diameter.

(19) The reaction between the reduced phase and the radical anion of the mediator could be possible following the process (III′) $[\text{Pt}_n^-, R_4N^+, R_4NBF_4] + M^{\bullet -} \rightarrow n\text{Pt} + M + 2R_4N^+ + BF_4^-$. The addition of this reaction with the reaction III results in reaction II, which is related to the regeneration of the mediator at the Pt substrate. The possibility of the occurrence of reaction III′ could explain the presence of the regeneration of the mediator above the modified area, and confirm that total negative feedback after the platinum reduction is not observed.

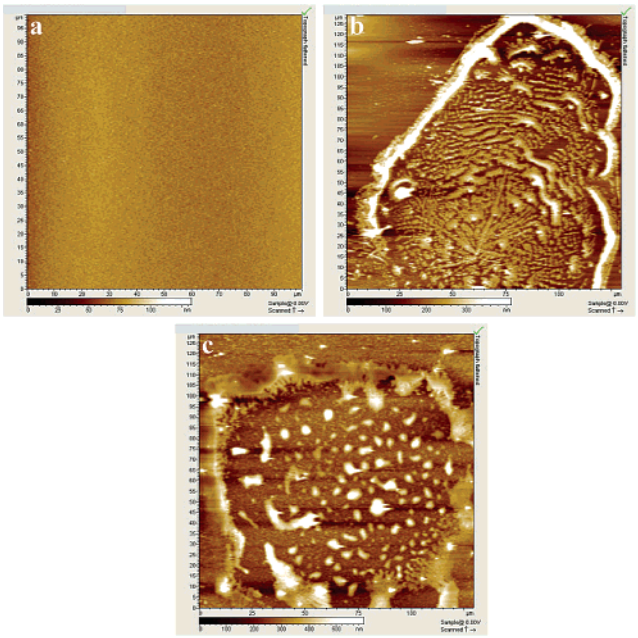

Figure 3. AFM images: (a) initial platinum substrate; (b,c) after modification using SECM in mode feedback, in the presence of naphthalene as mediator and tetrabutylammonium and tetraoctylammonium tetrafluoroborate, respectively. Scan size = 100 μm × 100 μm.

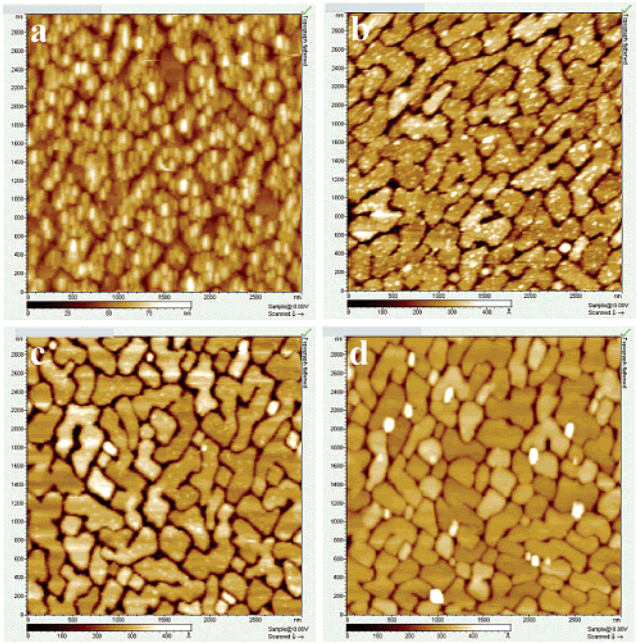

Figure 4. AFM images of the modified area for different distances from the center: (a) 0 μm, (b) 20 μm, (c) 40 μm, and (d) 60 μm. Scan size = 3 μm × 3 μm.

On the contrary, when the same experiments were performed with the less reducing radical anions, when $E°_{M/M^{\bullet-}}$ is more positive than E_T, no modifications of the surface were detected, confirming that no reaction with the platinum occurs and the same image as represented in Figure 3a is observed. In Figure 4, the local modification was examined in more detail at different locations, starting from the center of the modified area (decreasing the scan size). When the center of the modification is imaged, as shown in Figure 4a, the formation of small grains at the platinum surface is observed. The same topography was previously observed after direct electrochemical reduction of a platinum sample using EC-AFM.[10c] Figure 4 panels b and c show AFM images carried out at 20 and 40 μm far from the previous image, respectively.

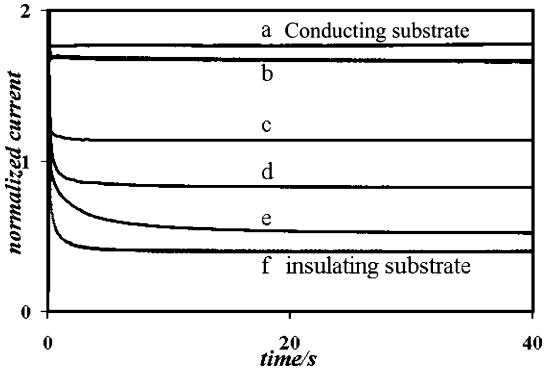

Figure 5. Variation of the transient normalized current as a function of time for different redox mediators at a fixed distance: (a) TCNQ, (b) nitrobenzene, (c) 4,4′-dipyridyl, (d) 2,2′-dipyridyl, (e) naphthalene, and (f) naphthalene above an insulating substrate. (Reference curve is for an insulating substrate.)

For both images, small grains are still observed above the platinum area, and the comparison between these two images evidences some progressive decreases of the grains density with the distance from the center. Finally, the image of Figure 4d recorded outside the modification, 60 μm away from the center, shows areas of platinum without any modification. These results demonstrate that the density of small grains, which is indicative of the platinum transformation, is much higher in the center of the modified area and considerably decreases for a distance between 0 and 40 μm, while no modifications are visible for distances larger than 40 μm.

Transient SECM Experiments. All these SECM experiments, described above, are performed in steady mode and thus provide little information about the kinetics of the process. To get more information about the kinetics of the transformation, SECM experiments were performed in transient mode.[20] The principle of the investigation is to apply a potential step at the tip electrode for producing a sort of burst of radical anions. During the experiments, the UME is maintained at a fixed distance L from the Pt substrate and the evolution of the normalized current is recorded versus the time (See Figure 5) for the different mediator couples in DMF solutions containing tetrabutylammonium salts. At the beginning of the potential step, the sample is freshly prepared and without any previous modification. Using the adapted procedure for adjusting the tip−substrate distance (see the experimental details), the adimensional parameter $L = d/a$ was tuned to be around 0.8, which provides a reasonable compromise between the error on the distance and the sensitivity of the measure.

As seen in Figure 5, all the currents reach time-independent values for experimental times > 20 s, which are in agreement with the previous steady state measurements. Moreover, the current recorded at the longest time (40 s) decreases with the reducing strength of the mediator radical anion, confirming the results obtained with the SECM approach curves. A second interesting observation concerns the time required for reaching the steady-state values, which increases for the strongest reducing agent. Thus, for the curve e (naphthalene radical anion),

(20) Fernández, J. L.; Bard, A. *J. Anal. Chem.* **2004**, *76*, 2281.

the current becomes stable only after 20 s, a time which is much longer than the characteristic time of a 10 μm radius UME tip. This result indicates that the variation of the current mainly reflects the transformations of the surface and not a change in the diffusion regime at the tip. After this 20 s duration, the reduced Pt phase has ceased to evolve and the steady-state current is observed.

Considering that point, we may use the formalism introduced by Bard−Mirkin for which the steady-state current I_s^k flowing through the Pt substrate can be estimated from the following equation as function of the normalized distance $L = d/a$:

$$I_T = I_s^k\left(1 - \frac{I_T^{ins}}{I_T^c}\right) + I_T^{ins} \quad (1)$$

Where I_T^c and I_T^{ins} are the normalized current tip for the diffusion-controlled regeneration and for an insulating surface, respectively.[21] They represent the two possible limiting behaviors, that is, the case where the regeneration of the mediator is infinitively fast and, on the opposite case, when no regeneration occurs (insulating substrate). For all mediators, our experimental curves were located between these two limiting behaviors. It is thus useful for characterizing the phenomena to consider the variations of I_s^k at a specified distance L (Figure 2D shows the current variation for $L = 0.1$) as a function of the standard potential of the redox mediators. As seen in Figure 2D, two different areas are clearly evidenced according to the reducing power of the radical anion electrogenerated at the UME. In the first area, corresponding to the mediators with a redox potential $E°_{M/M^{\bullet-}}$ more positive than −1.6 V/SCE, we observe that the current is independent of the mediator potential. In the second area (mediator d, e, and f), the logarithm of current varies linearly with the mediator reduction strength ($E°_{M/M^{\bullet-}}$). It is clear that the potential corresponding to the change of regime (intersection between the two areas) matches with the threshold potential of the Pt reduction wave, $E_{T,}$ observed in cyclic voltammetry. As discussed before, negligible or no modifications were detected with the three less negative redox couples located at the first area ($E°_{M/M^{\bullet-}} > -1.6$ V/SCE). Indeed, we found a good agreement between the experimental variations of I_T and the theoretical values calculated when the substrate current I_s^k is simply governed by the heterogeneous electron rate transfer kinetics. In such case, I_s^k depends on a single adimensional parameter $\kappa = k_{el}a/D$ where a is the electrode tip radius and D the diffusion coefficient of the mediator. We derived values around 0.2 cm·s^{-1} [21] that are in the range of the expected rates constants for such couples taking into account the "special" patterns of our platinum substrate.[22]

For the three most negative mediators ($E°_{M/M^{\bullet-}} < -1.6$ V), the situation appears more complicated as the morphological examination of the sample has shown that the Pt substrate is changing during the reduction process. Indeed, we failed to obtain a good fitting of our experimental data, according to the theoretical model described in the literature, on the basis of a simple electron-transfer law.[21] This result confirms that the negative feedback reflects both the decrease of the substrate conductivity and the evolution of the modification during the approach time. It remains that, even in the case of the most negative mediator (naphthalene/naphthalene radical anion), the approach curves are above the theoretical ones for nonconductive substrate, indicating that the layer was not totally insulating.[23] This complicated phenomenon could be compared with previously studied systems in which the transformation induces large changes in the conductivity in the case of PTFE (polytetrafluoroethylene).[24] To explain this occurrence, it is useful to consider the model previously proposed by Amatore et al.[25] that was originally developed for explaining the spatial extension of the mediated reduction of Teflon to carbonized Teflon in a microband setup. The basic idea is represented in Scheme 2. In a SECM setup, as the substrate is not electrically connected, the injection of negative charges under the ultramicroelectrode tip must be compensated by the inverse reaction outside the diffusion cone. At the beginning of the experiments, that is, on a conductive metallic electrode, this phenomenon is not limiting as the injected negative charges are rapidly evacuated outside the diffusion cone because the reverse reaction could occur on a much larger sample area (see Scheme 2A).

However, when the modification of Pt spreads out, the charge transport inside the materials becomes less facile in the modified area since the material is becoming insulating. Considering the Amatore's model, the rate of electron-transfer that controls I_s^k must exponentially depend on the locally available driving force. This driving force decreases while the layer extends because of the ohmic drop as the electrons must pass through a thicker and thicker layer (see Scheme 2B and C). Assuming a simple Buttler−Volmer law for the electron transfer kinetics, the local variations of the electron rate constants that characterize the reduction kinetics of the Pt to its insulating phase and of the mediator M to its radical anion, $k_{el,Pt}$ and $k_{el,M}$ respectively, at the border between the conductive and insulating areas for Pt and in the whole conductive area for the mediator are given by

(21) The kinetics of the transfer can be characterized by measuring the apparent electron transfer rate constant k_{el} using the formalism previously introduced by Mirkin and Bard. When interfacial electron transfer at the substrate/solution is the rate determining step, the normalized current I_T could be described by the following set of equations: $I_T = I_s^k(1 - I_T^{ins}/I_T^c) + I_T^{ins}$, $I_T^{ins} = (0.15 + 1.5358/L + 0.58\exp(-1.14L) + 0.0908\exp(L - 6.3/1.017L))^{-1}$, and $I_T^c = 0.68 + 0.78377/L + 0.3315\exp(-1.0672/L)$, where I_T^c, I_s^k, and I_T^{ins} are, respectively, the normalized current tip for the diffusion-controlled regeneration, for the kinetically limited electron transfer at the substrate interface, and for an insulating surface (see the preceding eq 1). I_s^k depends on a single adimensional parameter $k = k_{el}a/D$ where a is the electrode tip radius and D is the diffusion coefficient of the mediator. For $L > 2$ and $0.01 < k < 1000$, I_s^k can be approximated by the following equation: $I_s^k = 0.78377/(L(1 + 1/\Lambda)) + [0.68 + 0.3315\exp(-1.0672/L)/(1 + F(L,\Lambda))]$ with $F(L,\Lambda) = (11 + 7.3\Lambda)/(\Lambda(110 - 40L))$ and $\Lambda = \kappa L$.

(22) The sample involves numerous Pt pallets that are active sites with small size as compared to the diffusion layer dimensions. Under this condition, the electrochemical response of the system is the same as compared with an unblocked substrate, but with a decrease of the standard electron-transfer rate constant by a ratio $k'_{el} = k_{el}(1 - \varphi)$, where φ is the fractional coverage of the electrode by the blocking holes. Considering that the standard rate constant of the nitrobenzene/nitrobenzene radical anion is around 0.2 cm·s^{-1}, we derived a value of φ around 0.45 that is reasonable regarding the topography of our substrate. Amatore, C.; Saveant, J.-M.; Tessier, D. *J. Electroanal. Chem.* **1983**, *147*, 39.

(23) For the less negative mediators, the transient corresponds to a change in the diffusion regime of the ultramicroelectrode related to the geometry of the SECM.

(24) Combellas, C.; Kanoufi, F.; Mazouzi, D. *J. Phys. Chem. B* **2004**, *108*, 19260.

(25) (a) The reduction of Teflon to reduced carbon corresponds to the passage from insulating materials to conducting materials which is the inverse of our system. Despite this difference and a completely different chemistry, the general concept presented by C. Amatore et al. in reference 25b is the same than in our experimental situation.[25b] (b) Amatore, C.; Combellas, C.; Kanoufi, F.; Sella, C.; Thiebault, A.; Thouin, L. *Chem.—Eur. J.* **2000**, *6*, 820.

$$k_{el,Pt} = k^{o}_{el,Pt} \exp\{-\alpha[F(E_{border} - E^{\circ}_{Pt/Pt^{-}}) + \Theta I^{k}_{s} i^{\infty}_{T} R_{av}]/RT\} \quad (2)$$

and

$$k_{el,M} = k^{o}_{el,M} \exp\{-\alpha[F(E_{border} - E^{\circ}_{M}) + (1 - \Theta) I^{k}_{s} i^{\infty}_{T} R_{av}]/RT\} \quad (3)$$

where a is the transfer coefficient, E_{border} is the potential imposed by the mediator couple at the border between the conductive and insulating areas, $E^{\circ}_{M/M^{\bullet-}}$ and $E^{\circ}_{Pt/Pt^{-}}$ are the redox potentials, k^{o}_{el} are the values of k_{el} when $E_{border} = E^{\circ}$, Θ is the proportion of the current corresponding to the Pt reduction, and R_{av} is the average ohmic resistance of the modified platinum layer. $R_{av} = \rho l/S$, where l is the thickness of the modified platinum layer and S is the surface of the diffusion under the tip electrode. The thickness of the layer is proportional to the total charge passed through the platinum layer, leading to the transformation of Pt such as

$$R_{av} = A \int_0^t \Theta I^{k}_{s} \, dt$$

where A is a constant. Introducing the initial value of the electron rate transfer k^{i}_{el}, leading to the Pt transformation, that is, before the formation of the layer defined by $\log(k^{i}_{el,Pt}) = \log(k^{\circ}_{el,Pt}) - \alpha[F(E_{border} - E^{\circ}_{Pt/Pt^{-}})/RT]$, the equation could be rewritten as

$$k_{el,Pt} = k^{i}_{el,Pt} \exp[-A \int_0^t \Theta I^{k}_{s} \, dt]$$

$k_{el,Pt}$ characterizes the advancement of the Pt reduction but precise determination of A and Θ are difficult to obtain and required a full simulation of the process as Θ will vary with the time and space.[25b]

According to this treatment, three different situations could be described following the value of Θ ($0 \le \Theta \le 1$). The first situation is straightforward and corresponds to the case where $\Theta = 0$. In this case, $E^{\circ}_{M/M^{\bullet-}} > E_T$ which means that all the injected charge is used for the mediator regeneration and as consequence the Pt surface is not modified. The other limiting case is obtained when the $E^{\circ}_{M/M^{\bullet-}} \ll E_T$ ($\Theta = 1$), which corresponds to the situation where the whole charge is consumed for the Pt reduction. In such a case, simple estimations of k_{el} are possible, and through the eqs (1−2 and in reference 21), I^{k}_{s} that is proportional to the electronic rate constant, $k_{el,Pt}$, should rapidly tend to zero and the approach curves will be close to the one expected for an insulating surface. In summary, for these two limiting situations, when $\Theta = 0$, the approach curves show positive feedback, (conducting substrate) while total negative feedback (insulating case) should be observed in the case of $\Theta = 1$. The most general and interesting case corresponds to the intermediate situation, $0 < \Theta < 1$, that is, when the reducing power is strong enough to induce the Pt modification ($< E_T$) but not sufficiently to provoke the total modification of the Pt layer. In that case, the efficient potential at the conductive−insulating border, E_{border}, becomes less and less negative as the reduced Pt layer grows. The lateral evolution of the modified Pt is ended when E_{border} becomes more positive than E_T. After that, as seen in Figure 5, steady-state behaviors are due to the residual currents that originate from the reduction/oxidation of the mediator coupled with electron transport across the insulating surface (see Scheme 2C). This expected behavior is in agreement with the experimental data for $E^{\circ}_{M/M^{\bullet-}} < -1.6$ V where $\log(I^{k}_{s})$ varies linearly with the potential of the mediator $E^{\circ}_{M/M^{\bullet-}}$. The linear variation simply illustrates the competition between two redox processes: one is the reduction of the platinum and the second one is the ineffective redox reactions proper to the mediator. These two processes display different standard potentials and thus occur with a different driving force at the potential of the material. These expectations are confirmed by the AFM observation of the area after SECM experiments, where the quantity of reduced Pt (quantity of small grains) progressively decreases as soon as we are outside the diffusion cone of the tip UME. For applications related to local modifications or patterning of the Pt surface, we could deduce that the best spatial resolution will be obtained when the standard potential of the radical anion will be close to the E_T value.

Conclusion

The reduction of the Pt metal to form phases where Pt exists under negative oxidation states, is a general process in an organic dry solvent that is accompanied by large structural and chemical modifications. It occurs electrochemically when the metal is held at a negative potential as previously demonstrated. The present work demonstrates the possibility of reducing the Pt by the simple reaction of the metal in the presence of a organic reductant, like the radical-anion of an aromatic molecule. It is noticeable that the driving force required for this process is relatively mild. It starts with redox couples for which the standard potential $E^{\circ}_{M/M^{\bullet-}}$ is more negative than −1.6 V/SCE (at a more positive potential with an alkali metal). The exact value depends on the cation of the supporting electrolyte, but it is clear that the reaction is likely to occur with a large family of molecules. In such conditions, the extension of the reaction is rapidly limited by the passage from the metallic conducting Pt to the corresponding platinides which are insulating. If other redox reactions are possible, the "reduction of Pt" will interfere with these processes in a competition that depends on the standard potential of the reagent. More generally, the facility and the occurrence of this reaction should imply a great care in applications where the metallic Pt is in contact with some reductive agents and in the interpretation of any electrochemical data when using the material at high negative potentials.

Acknowledgment. The authors gratefully acknowledge the Agence Nationale de la Recherche for financial support (program N° ANR-05-BLAN-0003-04) of this research.

Supporting Information Available: Experiments describing the reaction of a Pt surface with a solution of naphthalene radical anion in DMF (AFM images and discussions);AFM images showing the Pt surfaces as the function of the electrochemical modification time. This material is available free of charge via the Internet at http://pubs.acs.org.

JA071483A